

# A virtual intersubband spin-flip spin-orbit coupling induced spin relaxation in GaAs (110) quantum wells

Y. Zhou<sup>1</sup> and M. W. Wu<sup>1,2,\*</sup>

<sup>1</sup>*Hefei National Laboratory for Physical Sciences at Microscale,  
University of Science and Technology of China, Hefei, Anhui, 230026, China*

<sup>2</sup>*Department of Physics, University of Science and Technology of China, Hefei, Anhui, 230026, China  
(Dated: November 8, 2018)*

A spin relaxation mechanism is proposed based on a second-order spin-flip intersubband spin-orbit coupling together with the spin-conserving scattering. The corresponding spin relaxation time is calculated via the Fermi golden rule. It is shown that this mechanism is important in symmetric GaAs (110) quantum wells with high impurity density. The dependences of the spin relaxation time on electron density, temperature and well width are studied with the underlying physics analyzed.

PACS numbers: 72.25.Rb; 71.70.Ej; 73.21.Fg

In recent years, semiconductor spintronics has become a focus of intense experimental and theoretical research [1, 2, 3, 4, 5, 6]. One of the key factors for the design of the spin-based device is to understand the spin relaxation such that the information is well preserved before required operations are completed. In  $n$ -type zinc-blende semiconductors, like GaAs, the leading spin relaxation mechanism in most situation is the D'yakonov-Perel' (DP) mechanism [7, 8, 9, 10], which is from the joint effects of the momentum scattering and the momentum-dependent effective magnetic field (inhomogeneous broadening [11, 12, 13]) induced by the Dresselhaus [15] and/or Rashba [16, 17] spin-orbit coupling (SOC). However, in symmetric (110)-oriented GaAs quantum wells (QWs), when only the lowest subband is occupied, the in-plane components of the spin-orbit field vanish and the effective magnetic field only exists along the growth direction [18]. As a result, electrons with spin polarization along the growth direction can not precess around the effective field, and therefore the DP mechanism is absent. It is also noted that in the presence of an in-plane external magnetic field, the in-plane and out-of-plane spin relaxations are mixed, thus the DP mechanism still leads to the spin relaxation/dephasing in this system, as point out by Wu and Kuwata-Gonokami [19]. Experimentally Ohno *et al.* [20] first observed very long spin relaxation time (SRT) in GaAs (110) QWs, which exceeds the SRT in (100) QWs by more than one order of magnitude. Later the spin dynamics in this system was studied by many works [21, 22, 23, 24, 25, 26, 27, 28, 29]. In most of these works, the main reason limiting the SRT is thought to be the Bir-Aronov-Pikus (BAP) mechanism [30, 31], which is due to the electron-hole exchange interaction (holes are from the optical excitation in  $n$ -type samples). In the spin noise spectroscopy measurements by Müller *et al.* [28], the excitation of semiconductor is negligible, and hence the BAP mechanism is avoided. They reported even longer SRT about 24 ns and attributed it to the DP mechanism due to the random Rashba fields caused by fluctuations in the donor den-

sity [32, 33]. In this note, we propose another spin relaxation mechanism to understand the slow spin relaxation in the *absence* of the DP and BAP mechanisms, which is based on a second-order spin-flip process of the intersubband SOC together with the spin-conserving scattering. We will show that this mechanism is important in symmetric GaAs (110) QWs with high impurity density.

We start our investigation from symmetrically doped GaAs (110) QWs with the growth direction along the  $z$ -axis. The well width is assumed to be small enough so that only the lowest subband is occupied for the temperature and electron density we discuss. The envelope functions of the relevant subband are calculated under the finite-well-depth assumption. The barrier layer is chosen to be  $\text{Al}_{0.39}\text{Ga}_{0.61}\text{As}$  where the barrier height is 328 meV [34]. The Hamiltonian can be written as ( $\hbar \equiv 1$ )

$$H = \sum_{nn'\mathbf{k}\sigma\sigma'} \left[ (\epsilon_{\mathbf{k}} + E_n) \delta_{nn'} \delta_{\sigma\sigma'} + \mathbf{h}^{nn'}(\mathbf{k}) \cdot \frac{\boldsymbol{\sigma}_{\sigma\sigma'}}{2} \right] \times c_{n\mathbf{k}\sigma}^\dagger c_{n'\mathbf{k}\sigma'} + H_I. \quad (1)$$

Here  $\epsilon_{\mathbf{k}} = k^2/2m^*$  is the energy spectrum of the electron with two-dimensional momentum  $\mathbf{k} = (k_x, k_y)$ ;  $E_n$  represents the quantized energy of the electron in the  $n$ -th subband;  $\boldsymbol{\sigma}$  is the Pauli matrix. In symmetric QWs without external gate voltage, the Rashba SOC can be neglected [35], and the spin-orbit field  $\mathbf{h}(\mathbf{k})$  is only from the Dresselhaus term. In the (110) coordinate system,  $\mathbf{h}(\mathbf{k})$  can be written as

$$\begin{aligned} h_x^{nn'}(\mathbf{k}) &= \gamma_D [-(k_x^2 + 2k_y^2) \langle n|k_z|n' \rangle + \langle n|k_z^3|n' \rangle], \\ h_y^{nn'}(\mathbf{k}) &= 4\gamma_D k_x k_y \langle n|k_z|n' \rangle, \\ h_z^{nn'}(\mathbf{k}) &= \gamma_D k_x (k_x^2 - 2k_y^2 - \langle n|k_z^2|n' \rangle) \delta_{nn'}, \end{aligned} \quad (2)$$

where  $\gamma_D = 30 \text{ eV} \cdot \text{\AA}^3$  denotes the Dresselhaus SOC coefficient [36] and  $\langle n|k_z^m|n' \rangle = \int dz \phi_n^*(z) (-i\partial/\partial z)^m \phi_{n'}(z)$  with  $\phi_n(z)$  representing the envelope function of the electron in  $n$ -th subbands. Since  $\langle n|k_z|n \rangle = \langle n|k_z^3|n \rangle = 0$ , all the in-plane components of the intersubband spin-orbit field vanish as mentioned above.

However,  $\langle 1|k_z|2\rangle \neq 0$ , thus the in-plane components of the intersubband spin-orbit field are still present. The interaction Hamiltonian  $H_I$  is composed of the electron-ionized-impurity, electron-longitudinal-optical (LO)-phonon, electron-acoustic (AC)-phonon and electron-electron Coulomb interactions. Their expressions can be found in textbooks [37, 38].

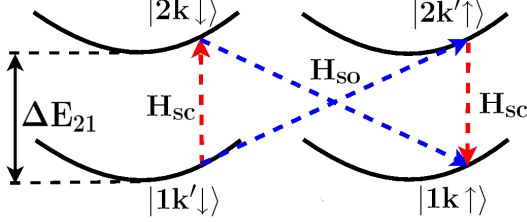


FIG. 1: (Color online) Schematic representation of a second-order spin-flip process based on the intersubband spin-orbit field  $H_{so}$  and the spin-conserving scattering  $H_{sc}$ .

A second-order spin-flip process can be constructed via the intersubband spin-orbit field and the spin-conserving scattering as depicted in Fig. 1. The matrix element of the spin-flip transition from the electron-impurity scattering (which is referred to as the spin-flip electron-impurity scattering in the following) is given by

$$U_{\uparrow\downarrow}(\mathbf{k}, \mathbf{k}', q_z) = \frac{\langle 1\mathbf{k}\uparrow | H_{so} | 2\mathbf{k}\downarrow \rangle \langle 2\mathbf{k}\downarrow | H_{ei}^{sc} | 1\mathbf{k}'\downarrow \rangle}{\epsilon_{\mathbf{k}'} - \epsilon_{\mathbf{k}} - \Delta E_{21}} + \frac{\langle 1\mathbf{k}\uparrow | H_{ei}^{sc} | 2\mathbf{k}'\uparrow \rangle \langle 2\mathbf{k}'\uparrow | H_{so} | 1\mathbf{k}'\downarrow \rangle}{-\Delta E_{21}}. \quad (3)$$

Here  $\Delta E_{21} = E_2 - E_1$  stands for the energy splitting between the first and second subbands of electrons. Although the above process is similar to the short-range Elliott-Yefet spin relaxation caused by virtual scattering [1, 39], the intermediate virtual states are chosen to be the states in the high conduction subband in stead of the states in the valence band in the previous work [39]. From the energy conservation  $\epsilon_{\mathbf{k}} = \epsilon_{\mathbf{k}'}$ , the symmetry of the form factor  $I_{12}(q_z) = I_{21}(q_z) = \langle 1|e^{iq_z z}|2\rangle$  and the symmetry of the spin-orbit field  $\mathbf{h}_{\parallel}^{21}(\mathbf{k}) = -\mathbf{h}_{\parallel}^{12}(\mathbf{k})$ ,  $U_{\uparrow\downarrow}(\mathbf{k}, \mathbf{k}', q_z)$  can be rewritten as

$$U_{\uparrow\downarrow}(\mathbf{k}, \mathbf{k}', q_z) = \frac{U_{\mathbf{k}'-\mathbf{k}} I_{12}(q_z)}{-\Delta E_{21}} [\mathbf{h}^{12}(\mathbf{k}) - \mathbf{h}^{12}(\mathbf{k}')] \cdot \boldsymbol{\sigma}_{\uparrow\downarrow}. \quad (4)$$

Similarly, one can obtain the matrix element of the spin-flip electron-phonon scattering

$$D_{\uparrow\downarrow}^{\eta}(\mathbf{k}, \mathbf{k}', q_z) = \frac{D_{\mathbf{Q}\eta} I_{12}(q_z)}{-\Delta E_{21}} [\mathbf{h}^{12}(\mathbf{k}) - \mathbf{h}^{12}(\mathbf{k}')] \cdot \boldsymbol{\sigma}_{\uparrow\downarrow}, \quad (5)$$

where  $\mathbf{Q} = (\mathbf{k}' - \mathbf{k}, q_z)$  is the three-dimensional momentum.  $U_{\mathbf{k}'-\mathbf{k}}$  and  $D_{\mathbf{Q}\eta}$  represent the matrix elements of the electron-impurity and electron-phonon interactions respectively, whose expressions are given in detail in

Ref. 40. From Eqs. (4) and (5), it is seen that the matrix elements of the spin-flip electron-impurity and electron-phonon scatterings are proportional to  $|\mathbf{h}^{12}(\mathbf{k}) - \mathbf{h}^{12}(\mathbf{k}')|/\Delta E_{21}$ . Thus the term containing  $k_z^3$  in  $\mathbf{h}(\mathbf{k})$ , which is independent of two-dimensional momentum  $\mathbf{k}$ , has no contribution to the spin-flip scattering.

By using the Fermi golden rule, the SRT is given by  $T_1^{-1} = T_1^{\text{ei}}{}^{-1} + T_1^{\text{ep}}{}^{-1}$  with [41]

$$T_1^{\text{ei/ep}}{}^{-1} = \frac{2 \sum_{\mathbf{k}\mathbf{k}'} \Gamma_{\uparrow\downarrow}^{\text{ei/ep}}(\mathbf{k}, \mathbf{k}', q_z) f_{\mathbf{k}}(1 - f_{\mathbf{k}'})}{\sum_{\mathbf{k}\mathbf{k}'} f_{\mathbf{k}}(1 - f_{\mathbf{k}'})}. \quad (6)$$

Here  $f_{\mathbf{k}}$  is the equilibrium electron distribution function.  $\Gamma_{\uparrow\downarrow}^{\text{ei/ep}}(\mathbf{k}, \mathbf{k}', q_z)$  represents the transition rate of the spin-flip electron-impurity or electron-phonon scattering, which can be written as

$$\Gamma_{\uparrow\downarrow}^{\text{ei}}(\mathbf{k}, \mathbf{k}', q_z) = 2\pi |U_{\uparrow\downarrow}(\mathbf{k}, \mathbf{k}', q_z)|^2 \delta(\epsilon_{\mathbf{k}} - \epsilon_{\mathbf{k}'}), \quad (7)$$

$$\Gamma_{\uparrow\downarrow}^{\text{ep}}(\mathbf{k}, \mathbf{k}', q_z) = 2\pi \sum_{\eta} |D_{\uparrow\downarrow}^{\eta}(\mathbf{k}, \mathbf{k}', q_z)|^2 [N_{\mathbf{Q}\eta} \delta(\epsilon_{\mathbf{k}} - \epsilon_{\mathbf{k}'} + \omega_{\mathbf{Q}\eta}) + (N_{\mathbf{Q}\eta} + 1) \delta(\epsilon_{\mathbf{k}} - \epsilon_{\mathbf{k}'} - \omega_{\mathbf{Q}\eta})]. \quad (8)$$

Here  $N_{\mathbf{Q}\eta}$  and  $\omega_{\mathbf{Q}\eta}$  are the distribution function and energy spectrum of the phonon with mode  $\eta$  and momentum  $\mathbf{Q}$ . It is noted that the spin relaxation process we discuss is only from the virtual intersubband scattering. The spin relaxation due to the real intersubband scattering [14, 24, 25] is negligible due to the small well width in the present investigation.

Our main results are summarized in Figs. 2–4. In Fig. 2, we plot the SRTs due to the spin-flip electron-impurity, electron-AC-phonon and electron-LO-phonon scatterings together with the total SRT with all the spin-flip scatterings included as function of temperature for  $N_i = N_e$  (solid curves) and  $N_i = 0.01 N_e$  (dashed curves).  $N_e = 1.8 \times 10^{11} \text{ cm}^{-2}$  and  $a = 16.8 \text{ nm}$ . In the low impurity density case with  $N_i = 0.01 N_e$ , it is seen that the spin relaxation due to the spin-flip electron-AC-phonon and spin-flip electron-impurity scatterings are comparable at low temperature and the contribution from the spin-flip electron-LO-phonon scattering becomes more important and even dominates at high temperature. In the high impurity density case with  $N_i = N_e$ , the spin relaxation due to the spin-flip electron-impurity scattering is dominant at most temperatures we discuss, and the contribution from the spin-flip electron-LO-phonon scattering becomes comparable to that from the spin-flip electron-impurity scattering when  $T > 80 \text{ K}$ .

We also compare our results with the experiment by Müller *et al.* [28] (square) in Fig. 2. By fitting the measured mobility given in Ref. 28, one obtains  $N_i \sim 0.01 N_e$ . In this case, it is seen that the SRT obtained from our model is two orders of magnitude larger than the experimental data at  $T = 20 \text{ K}$ . However, in the high impurity case with  $N_i = N_e$ , it is shown that the spin relaxation

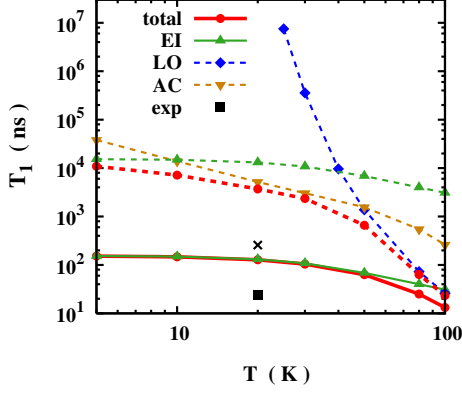


FIG. 2: (Color online) SRTs due to the spin-flip electron-impurity, electron-AC-phonon and electron-LO-phonon scatterings as well as the total SRT with all the spin-flip scatterings included *vs.* temperature  $T$  with well width  $a = 16.8$  nm and electron density  $N_e = 1.8 \times 10^{11} \text{ cm}^{-2}$ . The impurity densities are  $N_i = N_e$  (solid curves) and  $0.01 N_e$  (dashed curves), respectively. The square represents the experimental result in Ref. 28. The cross represents the SRT due to the RRDP mechanism for  $N_i = N_e$ , calculated via the relation  $T_1^{\text{RRDP}} \propto 1/\tau_p$ .

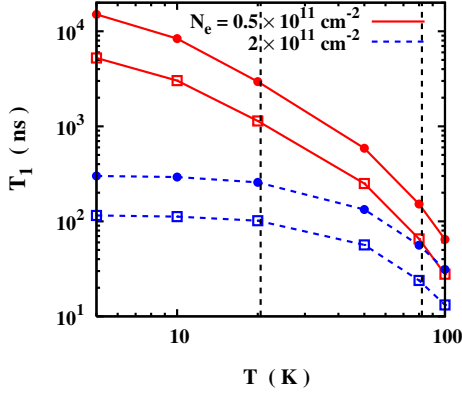


FIG. 3: (Color online) SRTs with all the spin-flip scatterings included *vs.* temperature  $T$  for  $N_i = N_e = 0.5 \times 10^{11} \text{ cm}^{-2}$  and  $2 \times 10^{11} \text{ cm}^{-2}$ , respectively. The well widths are  $a = 10$  nm ( $\bullet$ ) and  $16.8$  nm ( $\square$ ). The black dashed vertical lines indicate the Fermi temperatures  $T_F^e$  for both electron densities.

rate due to our mechanism is enhanced by more than one order of magnitude. Meanwhile, the spin relaxation rate due to the random Rashba field induced DP (RRDP) mechanism [32, 33] is suppressed significantly due to the increase of the electron-impurity scattering. Here we estimate the SRT due to the RRDP mechanism at  $N_i = N_e$  (cross) by using the relation  $T_1^{\text{RRDP}} \propto 1/\tau_p$  [1]. It is seen that the mechanism from our model becomes more im-

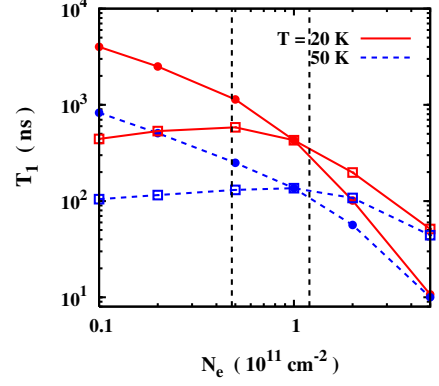


FIG. 4: (Color online) SRTs with all the spin-flip scatterings included *vs.* electron density  $N_e$  for temperatures  $T = 20$  K and  $50$  K, with impurity densities  $N_i = N_e$  ( $\bullet$ ) and  $N_i = 10^{11} \text{ cm}^{-2}$  ( $\square$ ). The black dashed vertical lines indicate the electron densities satisfying  $E_F^e = k_B T$  for both temperatures.

portant compared with the RRDP mechanism in the high impurity case.

Now we discuss the temperature dependence of the SRT. In Fig. 3 we plot the SRT as function of temperature for different electron densities and well widths. It is shown that the SRT first decreases slowly and then rapidly with  $T$ . The turning point is roughly around the electron Fermi temperature  $T_F^e = E_F^e/k_B$ . Since the electron-impurity scattering has a weak temperature dependence, the temperature dependence of the SRT is mainly from the  $k$ -dependent spin-orbit field  $\mathbf{h}(\mathbf{k})$ . From Eqs. (4) and (5), it is seen that only the quadratic terms in  $\mathbf{h}(\mathbf{k})$  contribute to the spin-flip scattering. When temperature increases, more electrons are distributed at larger momentum states, and then the contribution from  $\mathbf{h}(\mathbf{k})$  becomes larger. This leads to a larger spin-flip scattering rate and hence reduces the SRT. It is also noted the average momentum of electrons is not sensitive to temperature in the degenerate regime ( $T < T_F^e$ ). Thus the SRT decreases slowly at low temperature. From Fig. 3, it is also seen that the SRT becomes shorter for wider well width. It can be understood as follows. Since the form factor is weakly dependent on well width, one obtains that  $T_1 \propto (\Delta E_{21}/\langle 1/k_z | 2 \rangle)^2$  from Eqs. (4)–(8). It is known that  $\Delta E_{21} \propto a^{-2}$  and  $\langle 1/k_z | 2 \rangle \propto a^{-1}$  under the infinite well-depth assumption. Thus the SRT decreases with an increase of well width.

The electron density dependence of the SRT is also investigated. In Fig. 4, the SRT is plotted as function of electron density for different temperatures and impurity densities. We first discuss the case with fixed impurity density  $N_i = 10^{11} \text{ cm}^{-2}$ . It is seen that the SRT first increases and then decreases with  $N_e$  with a peak around the electron density satisfying  $E_F^e = k_B T$ . This peak originates from the competition of two effects. On one

hand, similar to the discussion in temperature dependence, with the increase of electron density, the average  $k$  increases and thus the contribution from  $\mathbf{h}(\mathbf{k})$  is enhanced. This effect leads to a decrease of the SRT. On the other hand, the screening of electrons also increases with electron density, which suppresses the spin-flip scattering and increases the SRT. When the electron density is low and  $E_F^e < k_B T$ , i.e., in the nondegenerate regime, the average  $k$  changes little with  $N_e$ . Thus the effect of the increase in the screening is dominant and the SRT increases with increasing density. However, when the electron density is high enough so that  $E_F^e > k_B T$ , i.e., in the degenerate regime, the effect of the increase of the contribution from  $\mathbf{h}(\mathbf{k})$  becomes more important. Consequently the SRT decreases. Then we turn to the case with  $N_i = N_e$ . It is seen that the SRT decreases monotonically with electron density. This is because the effect of the increase of the impurity scattering surpasses the one of the increase of screening, and makes the SRT decrease even in low electron density (nondegenerate) regime. Nevertheless, one still can see that the SRT decreases more rapidly in the degenerate regime.

In conclusion, we have proposed a spin relaxation mechanism based on a second-order spin-flip process of the intersubband spin-flip SOC and the spin-conserving scattering, and calculated the corresponding SRT via the Fermi golden rule. We show that this mechanism is important in symmetric GaAs (110) QWs with high impurity density. The temperature, well width and electron density dependences of the SRT are also investigated.

This work was supported by the National Natural Science Foundation of China under Grant No. 10725417, the National Basic Research Program of China under Grant No. 2006CB922005 and the Knowledge Innovation Project of Chinese Academy of Sciences. We thank M. Q. Weng for valuable discussions.

---

\* Author to whom correspondence should be addressed; Electronic address: mwwu@ustc.edu.cn.

- [1] F. Meier, B.P. Zakharchenya (Eds.), *Optical Orientation*, North-Holland, Amsterdam, 1984.
- [2] S.A. Wolf, D.D. Awschalom, R.A. Buhrman, J.M. Daughton, S. von Molnár, M.L. Roukes, A.Y. Chtchelkanova, D.M. Treger, *Science* 294, (2001) 1488.
- [3] D.D. Awschalom, D. Loss, N. Samarth (Eds.), *Semiconductor Spintronics and Quantum Computation*, Springer-Verlag, Berlin, 2002.
- [4] I. Žutić, J. Fabian, S. Das Sarma, *Rev. Mod. Phys.* 76, (2004) 323.
- [5] J. Fabian, A. Matos-Abiague, C. Ertler, P. Stano, I. Žutić, *Acta Phys. Slov.* 57, (2007) 565.
- [6] M.I. D'yakonov (Ed.), *Spin Physics in Semiconductors*, Springer, Berlin, 2008.
- [7] M.I. D'yakonov, V.I. Perel', *Zh. Eksp. Teor. Fiz.* 60, (1971) 1954.
- [8] M.I. D'yakonov, V.I. Perel', *Sov. Phys. JETP* 33, (1971) 1053.
- [9] M.I. D'yakonov, V.I. Perel', *Fiz. Tverd. Tela* 13, (1971) 3581.
- [10] M.I. D'yakonov, V.I. Perel', *Sov. Phys. Solid State* 13, (1972) 3023.
- [11] M.W. Wu, C.Z. Ning, *Eur. Phys. J. B* 18, (2000) 373.
- [12] M.W. Wu, *J. Phys. Soc. Jpn.* 70, (2001) 2195.
- [13] M.Q. Weng, M.W. Wu, *Phys. Rev. B* 68, (2003) 075312.
- [14] M.Q. Weng, M.W. Wu, *Phys. Rev. B* 70, (2004) 195318.
- [15] G. Dresselhaus, *Phys. Rev.* 100, (1955) 580.
- [16] Y.A. Bychkov, E.I. Rashba, *J. Phys. C* 17, (1984) 6039.
- [17] Y.A. Bychkov, E.I. Rashba, *JETP Lett.* 39, (1984) 78.
- [18] R. Winkler, *Phys. Rev. B* 69, (2004) 045317.
- [19] M.W. Wu, M. Kuwata-Gonokami, *Solid State Commun.* 121, (2002) 509.
- [20] Y. Ohno, R. Terauchi, T. Adachi, F. Matsukura, H. Ohno, *Phys. Rev. Lett* 83, (1999) 4196.
- [21] Y. Ohno, R. Terauchi, T. Adachi, F. Matsukura, H. Ohno, *Physica E* 6, (2000) 817.
- [22] T. Adachi, Y. Ohno, F. Matsukura, H. Ohno, *Physica E* 10, (2001) 36.
- [23] O.Z. Karimov, G.H. John, R.T. Harley, W.H. Lau, M.E. Flatté, M. Henini, R. Airey, *Phys. Rev. Lett* 91, (2003) 246601.
- [24] S. Döhrmann, D. Hägele, J. Rudolph, M. Bichler, D. Schuh, M. Oestreich, *Phys. Rev. Lett* 93, (2004) 147405.
- [25] D. Hägele, S. Döhrmann, J. Rudolph, M. Oestreich, *Adv. Solid State Phys.* 45, (2005) 253.
- [26] P.S. Eldridge, W.J.H. Leyland, P.G. Lagoudakis, O.Z. Karimov, M. Henini, D. Taylor, R.T. Phillips, R.T. Harley, *Phys. Rev. B* 77, (2008) 125344.
- [27] V.V. Bel'kov, P. Olbrich, S.A. Tarasenko, D. Schuh, W. Wegscheider, T. Korn, C. Schüller, D. Weiss, S.D. Ganichev, *Phys. Rev. Lett* 100, (2008) 176806.
- [28] G.M. Müller, M. Römer, D. Schuh, W. Wegscheider, J. Hübner, M. Oestreich, *Phys. Rev. Lett* 101, (2008) 206601.
- [29] P. Olbrich, J. Allerdings, V.V. Bel'kov, S.A. Tarasenko, D. Schuh, W. Wegscheider, T. Korn, C. Schüller, D. Weiss, S.D. Ganichev, *Phys. Rev. B* 79, (2009) 245329.
- [30] G.L. Bir, A.G. Aronov, G.E. Pikus, *Zh. Eksp. Teor. Fiz.* 69, (1975) 1382.
- [31] G.L. Bir, A.G. Aronov, G.E. Pikus, *Sov. Phys. JETP* 42, (1976) 705.
- [32] E.Y. Sherman, *Appl. Phys. Lett.* 82, (2003) 209.
- [33] E.Y. Sherman, *Phys. Rev. B* 67, (2003) 161303(R).
- [34] E.T. Yu, J.O. McCaldin, T.C. McGill, *Solid State Phys.* 46, (1992) 1.
- [35] Bernardes et al. [E. Bernardes, J. Schliemann, M. Lee, J.C. Egues, D. Loss, *Phys. Rev. Lett.* 99, (2007) 076603; see also R. S. Calsaverini, E. Bernardes, J.C. Egues, D. Loss, *Phys. Rev. B* 78, (2008) 155313] showed that the inter-subband Rashba SOC is nonzero even in symmetric QWs due to the distinct parities of the envelope functions in different subbands. However, since the band gap of GaAs is about two times larger than that of  $\text{Ga}_{0.47}\text{In}_{0.53}\text{As}$  which is discussed in those papers, the corresponding Rashba coefficient is about four times smaller than that in  $\text{Ga}_{0.47}\text{In}_{0.53}\text{As}$ . For the cases we discuss, the corresponding SRT from the inter-subband Rashba SOC is one order of magnitude larger than that from the Dresselhaus SOC and is therefore negligible.
- [36] U. Rössler, *Solid State Commun.* 49, (1984) 943.

- [37] G.D. Mahan, Many-Particle Physics, Plenum, New York, 1981.
- [38] H. Haug, A.P. Jauho, Quantum kinetics in Transport and Optics of Semiconductors, Springer, Berlin, 1998.
- [39] E.L. Ivchenko, S.A. Tarasenko, JETP 99, (2004) 379.
- [40] J. Zhou, M.W. Wu, Phys. Rev. B 77, (2008) 075318.
- [41] The matrix elements of the spin-flip electron-electron Coulomb scattering are proportional to  $[\mathbf{h}^{12}(\mathbf{k}) -$

$\mathbf{h}^{12}(\mathbf{k}')]/\Delta E_{21}]^2$ , while the matrix elements of the spin-flip electron-impurity and electron-phonon scatterings are proportional to  $|\mathbf{h}^{12}(\mathbf{k}) - \mathbf{h}^{12}(\mathbf{k}')|/\Delta E_{21}$ . In the parameter regime we discuss,  $|\mathbf{h}^{12}(\mathbf{k}) - \mathbf{h}^{12}(\mathbf{k}')|/\Delta E_{21} < 0.01$ . Consequently, the contribution from the spin-flip electron-electron Coulomb scattering is negligible.